Dark gas contribution to diffuse gamma-ray emission

Masaki Mori

ICRR CANGAROO group internal seminar, November 7, 2005

25 February 2005

Dark Matter Need Not Apply

Adrian Cho

The Milky Way galaxy may be held together by plain old ordinary matter after all. New research indicates that the space between stars contains twice as much cold gas as previously thought. If so, the gas might provide enough gravity to keep the galaxy from flying apart, eliminating the need for mysterious dark matter.

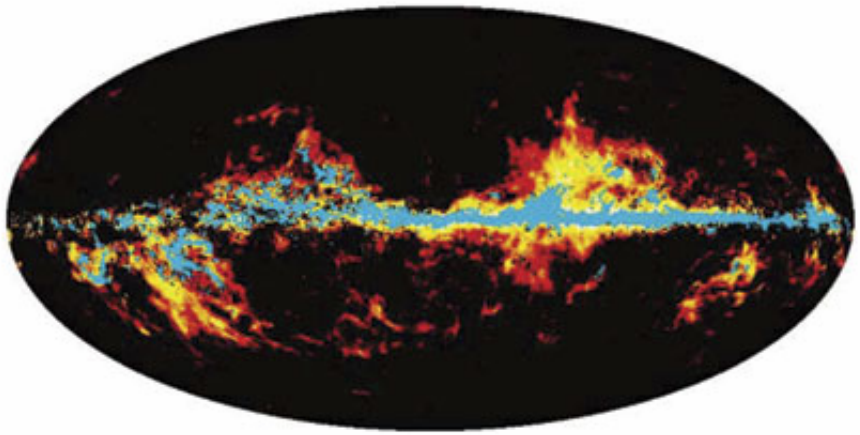

There all along. In the solar neighborhood, clouds of cold, dark gas (yellow and red) appear to surround clouds of molecular hydrogen (blue).
CREDIT: Grenier *et al*, *Science*

The matter strewn through interstellar space consists mostly of hydrogen. Nearly all of this comes in two forms: Relatively warm clouds of individual hydrogen atoms and colder clouds of diatomic molecules. Researchers measure the amount of warmer atomic hydrogen by tracking radio waves emitted by the atoms. But to spot the colder hydrogen, which emits no easily detectable signal, researchers must measure radio waves emitted by carbon monoxide and assume that the two molecules are found together in a certain ratio. Using such measurements, astrophysicists have estimated the amount of mass in our galaxy and come up with a value too small to generate enough gravity to prevent the outermost stars from whizzing into space. So researchers generally believe that some form of undetected dark matter must provide the extra gravity.

The Galactic Diffuse Gamma-ray Emission

... the dominant feature of the gamma-ray sky and
a probe of the *Galactic ISM* and the *CR distributions*

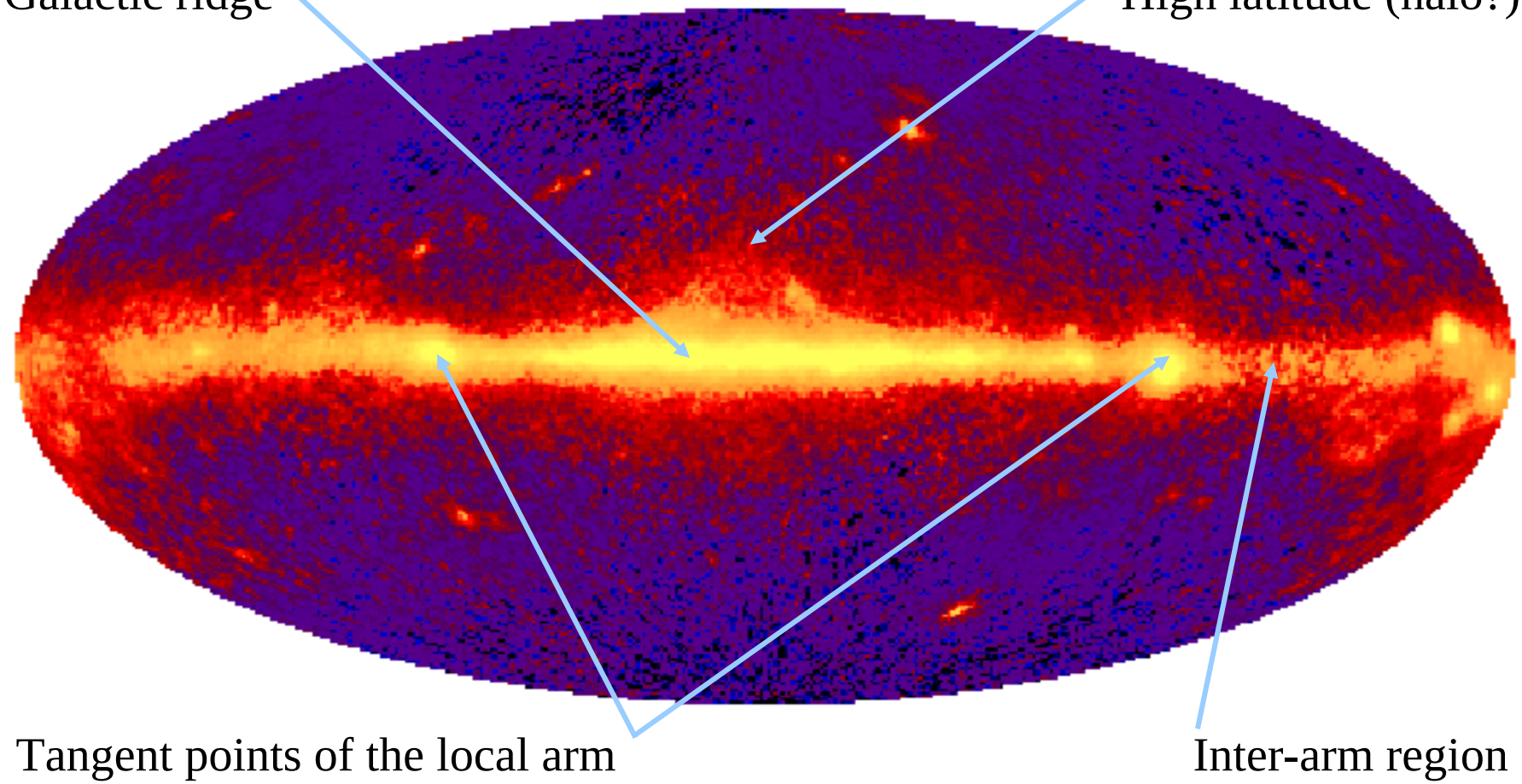

The Galactic Diffuse Emission

Straight forward integral over the line-of-sight:

Galactic cosmic-ray distribution of electrons and nucleons (+ He, heavies)

Galactic matter distribution of atomic, molecular, and ionized hydrogen

$$j(E_\gamma, l, b) = \frac{1}{4\pi}\int (c_e \cdot q_{eb} + c_n \cdot q_{nn}) \times (n_{\mathrm{H\,I}} + n_{H2} + n_{\mathrm{H\,II}})\, \mathrm{d}\rho +$$

$$\frac{1}{4\pi}\sum_i \int c_e \cdot q_{ic,i} \cdot u_{ic,i}\, \mathrm{d}\rho \quad [\mathrm{ph\ cm^{-2}\ s^{-1}\ sr^{-1}\ GeV^{-1}}]$$

Gamma-ray production functions electron bremsstrahlung, nucleon-nucleon (π^o), and inverse Compton
Synchrotron emission is not significant

Low-energy photon energy density cosmic microwave background, infra-red, visible, and ultraviolet

The hard part: determining the 3-D matter, ISR, and CR distributions.

Composition of the ISM - Matter & Radiation

- Interstellar Clouds $0.011 M_\odot / pc^3$, ~90% of ISM
  - Bright Nebulae, e.g. Orion (M42)
  - HI 8 H-atoms/cm^3, 0.01 elec/cm^3
  - All other elements
  - Dark Nebulae, e.g. Ophiuchus
  - H_2 1 H-mol/cm^3
  - HII ~8 elec/cm^3
- Interstellar Gas
  - Mean density between clouds — 0.1 H-atoms/cm^3, 0.035 elec/cm^3
- Interstellar Grains $0.0015 M_\odot / pc^3$, ~10% of ISM
  - Number density 0.5×10^{-12} cm^{-3} — Mass density ~1g/cm^3
- Stellar radiation — 7×10^{-13} erg/cm^3
  - CMB (2.7°K) — 4×10^{-13} erg/cm^3
    - Turbulent gas motion — 5×10^{-13} erg/cm^3
    - Cosmic rays — 16×10^{-13} erg/cm^3
    - Magnetic field — 15×10^{-13} erg/cm^3
- *Should this list also include dark matter?*

Gas Distribution

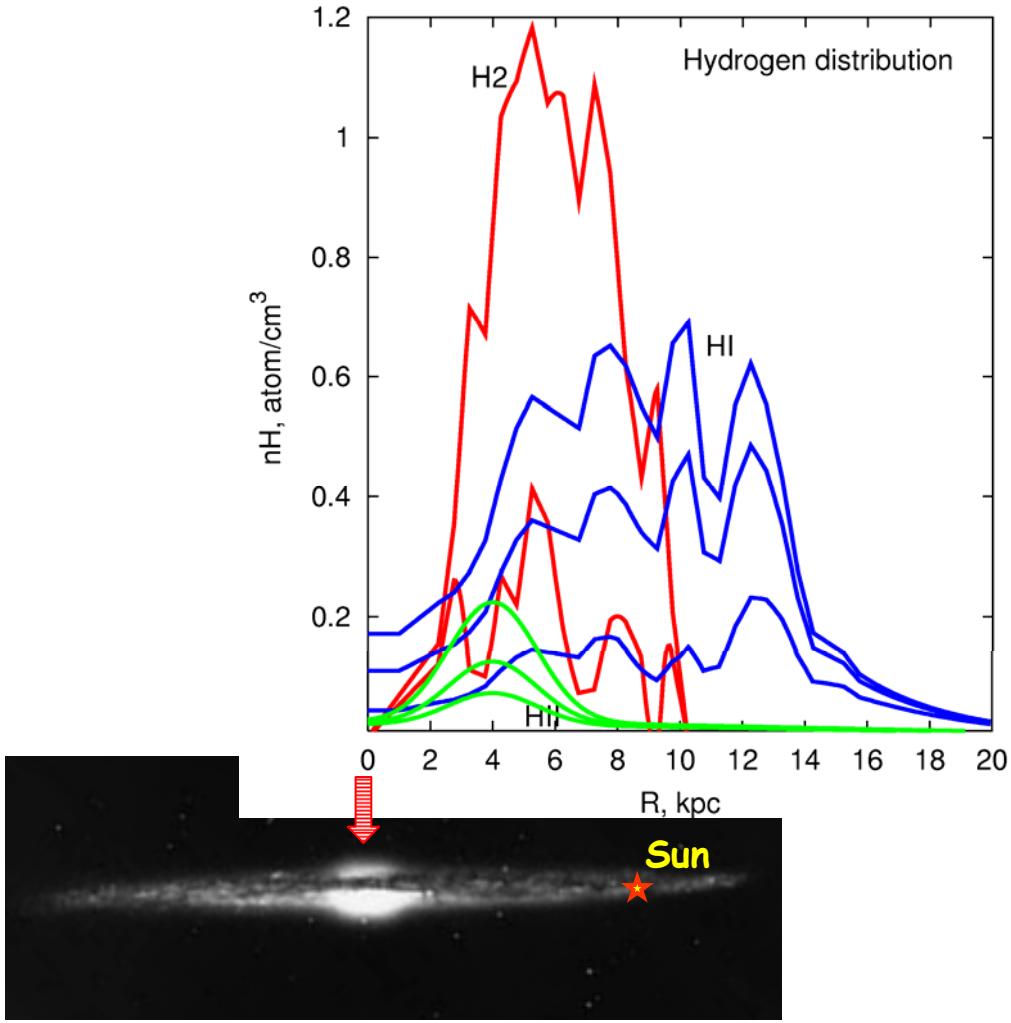

Molecular hydrogen H_2 is traced using J=1-0 transition of ^{12}CO, concentrated mostly in the plane (z~70 pc, R<10 kpc)

Molecular mass ratio: $X=N(H_2)/W_{CO}$

Atomic hydrogen H I has a wider distribution (z~1 kpc, R~30 kpc)

Ionized hydrogen H II – small proportion, but exists even in halo (z~1 kpc)

CR Distribution from Dynamic Balance

- Derive 3-D distributions of HI, H_2, and HII
- Determine Galactic mater surface density, normalize total Solar density to unity,

$$c_e = c_n = c(l,\rho)$$

- CR density at l,ρ is then Solar CR density $\times$ $c(l,\rho)$
- The diffuse emission is $\propto$ (Matter density)^2
- CR scale height assumed to be large compared to matter scale height

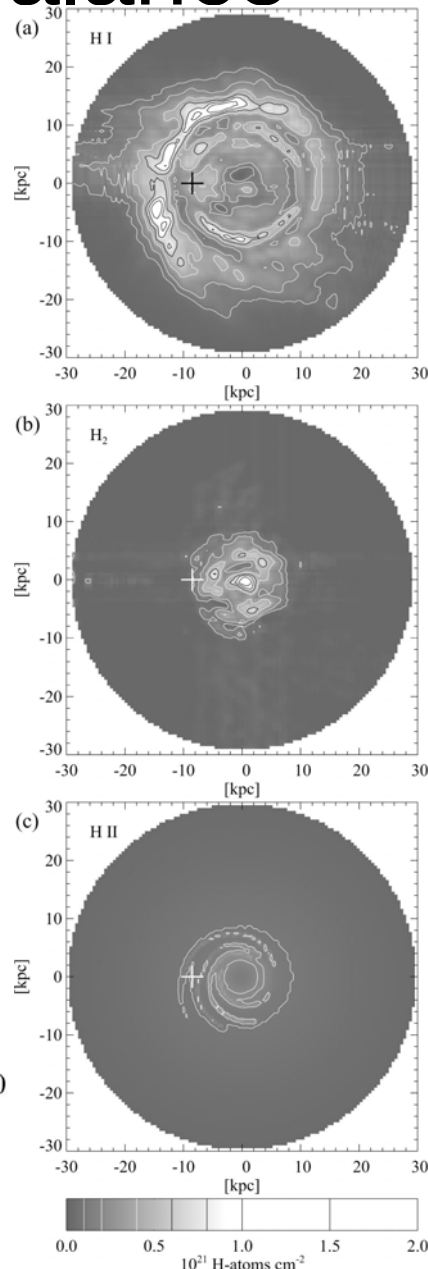

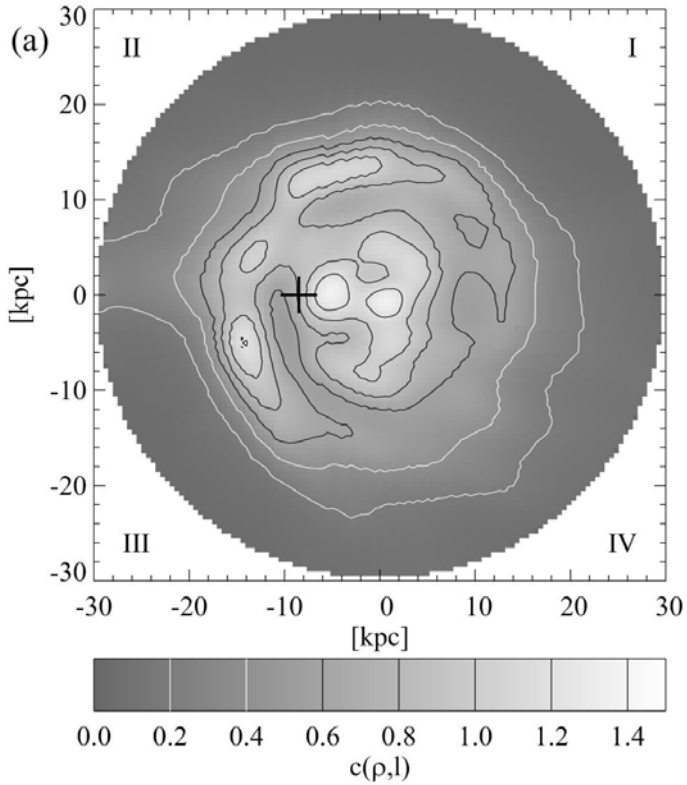

Interstellar radiation field

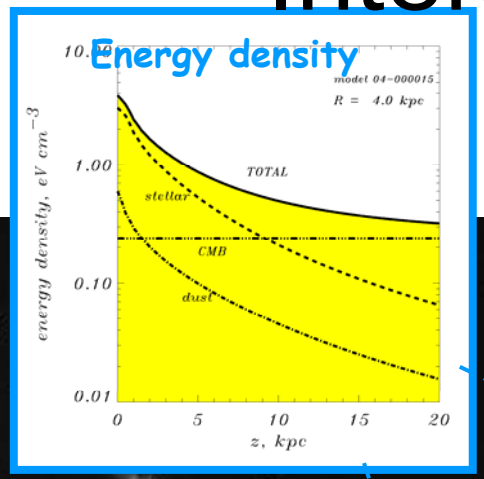

- Stellar
- Dust
- CMB

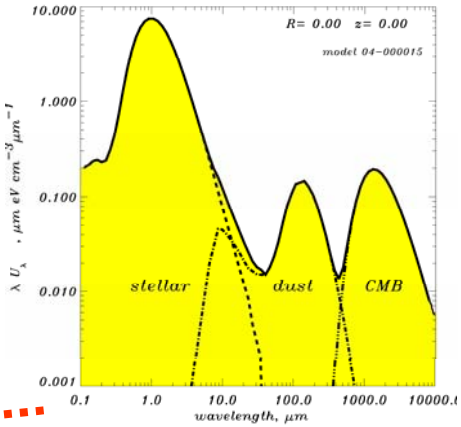

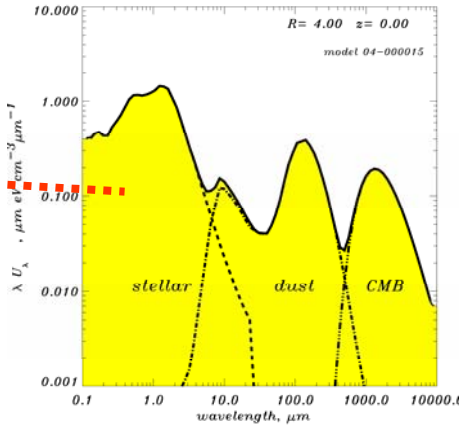

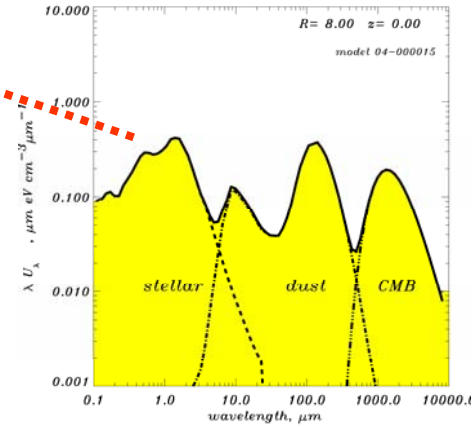

Sun

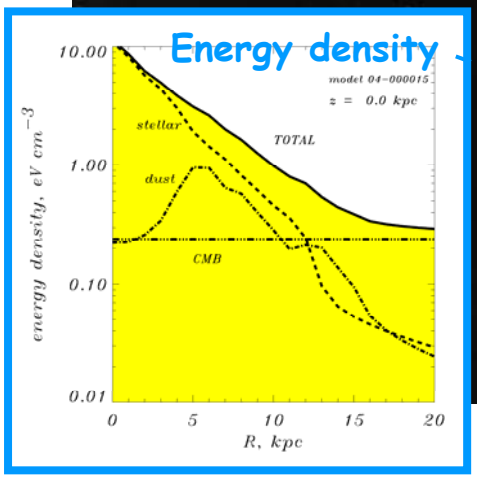

S. Hunter, GLAST meeting, Oct.2004

Comparison with EGRET data

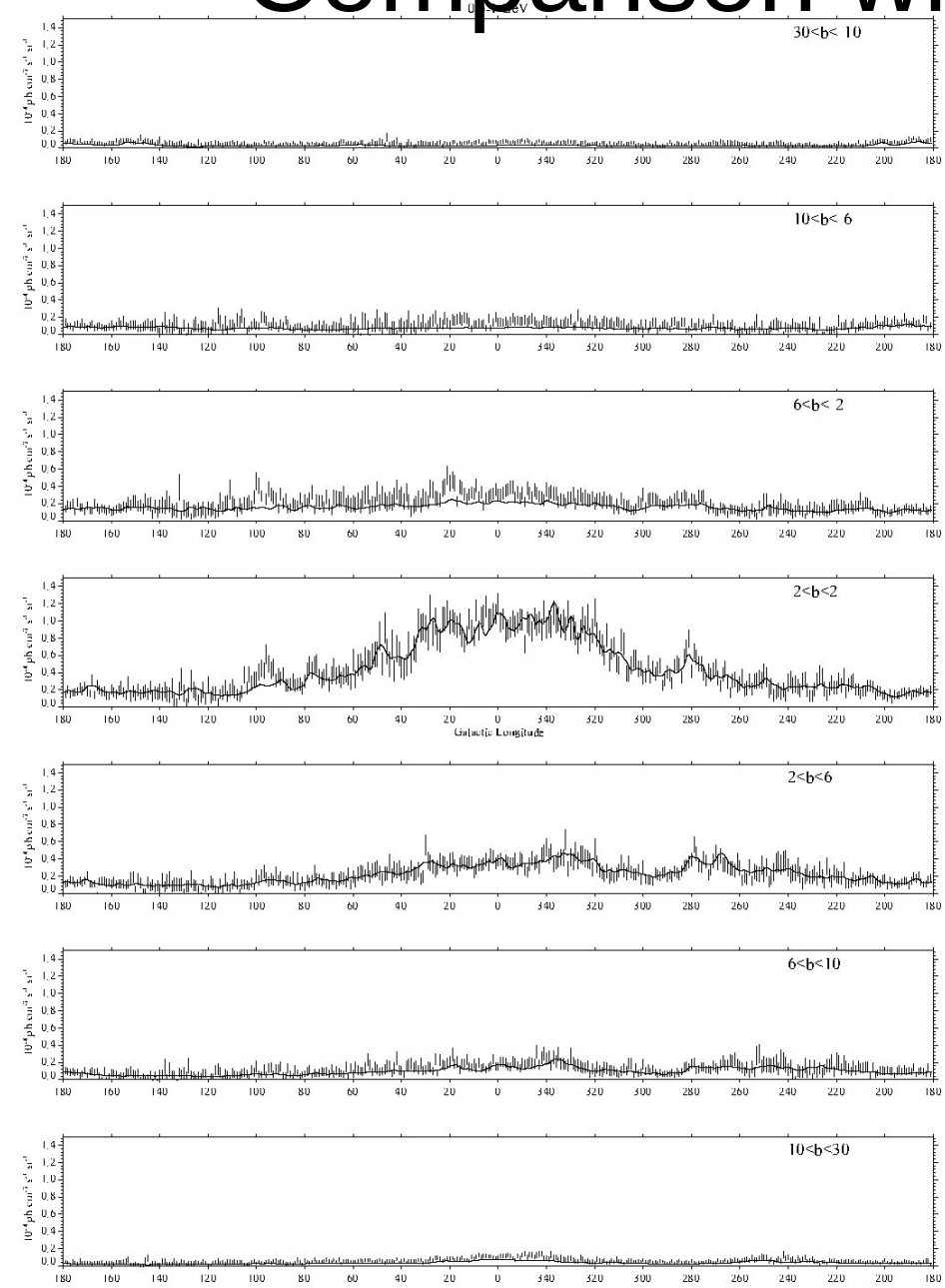

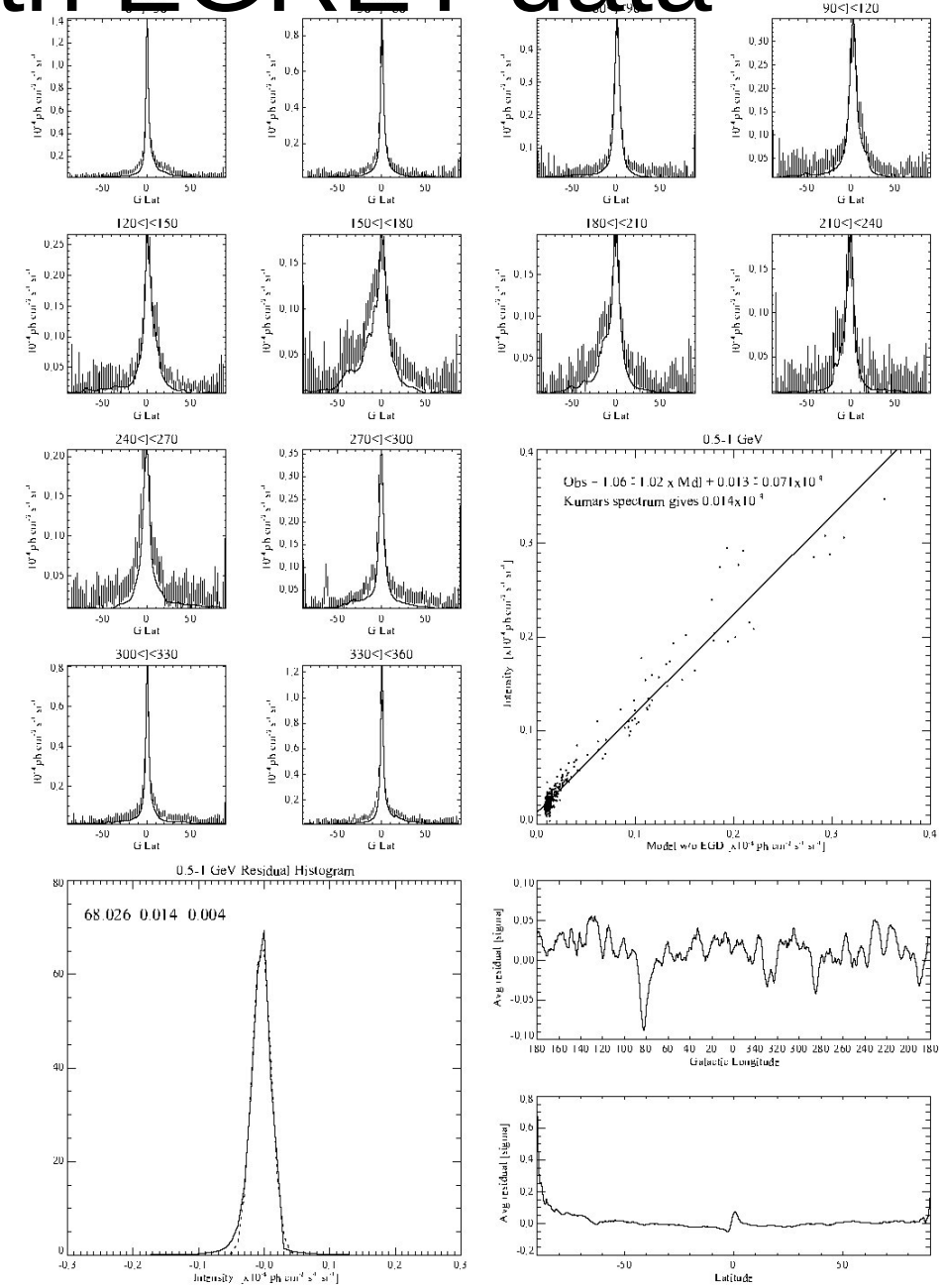

Grenier, Casandjian & Terrier, Science 307, 1292 (2005)

Dark gas contribution

- Additional $q_{\rm dust} I_{\rm dust}(l,b)$ term
- Possible dust intensity maps:
  - E(B-V): reddening map
    - I_{3000}, IRAS 3000 GHz map, corrected to 18.2K with use of DIRBE 100-240μm ratios
  - I_{94}: intensity map at 94 GHz
    - COBE DMR/FIRAS

Grenier, Casandjian & Terrier, Science 307, 1292 (2005)

Map of “excess dust reddening” = dark gas?

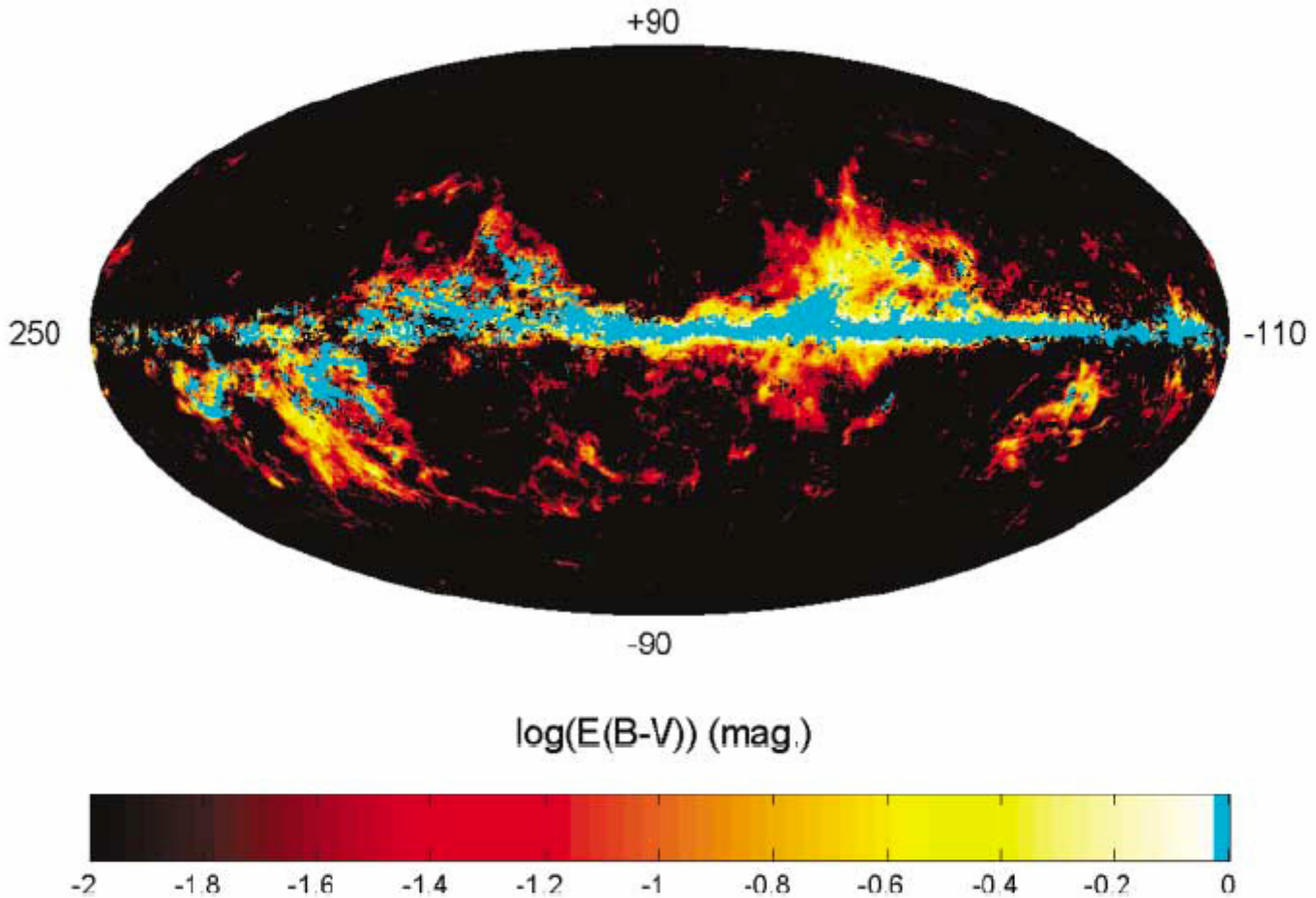

Fig. 1. Map, in Galactic coordinates centered on $l = 70°$, of the excess dust reddening found above that linearly correlated with the integrated HI and CO line intensities. The 94-GHz emission map shows the same excesses. CO intensities above 4 K km s^{-1} are overlaid in cyan. The dust excesses form extended halos around all CO clouds, the bright ones as well as the fainter CO cloudlets that are not overlaid. This dust spreads in a dark gas, not seen in HI and CO but detected in γ rays.

Grenier, Casandjian & Terrier, Science 307, 1292 (2005)

Best fits to diffuse gamma-ray data

Table 1. Best fits to the γ-ray data at $5° \leq |b| \leq 80°$ and $10° \leq |b| \leq 80°$, for the complete and residual (in bold and italics) dust maps. The log-likelihood ratios 2.ln(λ), measuring the fit improvement, are given with respect to the N(HI)+W(CO) gas model and are distributed as a χ^2 with one degree of freedom (*12*). The errors are statistical, not including systematic uncertainties [10% in the EGRET exposure (*10*), 20% in the true N(HI) (*32*) and dust maps (*5*), and 20% in the "dust-free" q_{CO} because of cloud-to-cloud variations in the dust residuals toward the CO clouds].

2.ln(λ)	q_{HI} (10^{-26} s^{-1} sr^{-1})	q_{CO} (10^{-6} cm^{-2} sr^{-1} K^{-1} km^{-1})	q_{EBV} (10^{-6} mag^{-1} cm^{-2} s^{-1} sr^{-1})	q_{I94} (10^{-4} mK^{-1} cm^{-2} s^{-1} sr^{-1})	q_{I3000} (10^{-7} MJy^{-1} cm^{-2} s^{-1})	q_{IC} (10^{-1})	q_{SOU}	I_E (10^{-6} cm^{-2} s^{-1} sr^{-1})
				$5° \leq \|b\| \leq 80°$				
0	1.62 ± 0.01	5.65 ± 0.10				7.46 ± 0.06	1.01 ± 0.01	13.21 ± 0.09
241.8	***1.63 ± 0.01***	***5.54 ± 0.09***			***2.83 ± 0.20***	***6.54 ± 0.09***	***1.00 ± 0.01***	***13.93 ± 0.10***
1298.0	***1.64 ± 0.01***	***5.82 ± 0.09***		***4.27 ± 0.12***		***6.39 ± 0.07***	***0.96 ± 0.01***	***13.96 ± 0.09***
1556.7	***1.65 ± 0.01***	***5.91 ± 0.09***	***57.5 ± 1.5***			***6.43 ± 0.07***	***0.96 ± 0.01***	***13.91 ± 0.09***
241.8	1.49 ± 0.02	4.84 ± 0.11			2.83 ± 0.21	6.54 ± 0.09	1.00 ± 0.01	13.74 ± 0.10
1298.0	0.77 ± 0.02	1.63 ± 0.15		4.27 ± 0.10		6.39 ± 0.07	0.96 ± 0.01	14.30 ± 0.09
1556.7	0.71 ± 0.04	0.53 ± 0.54	57.5 ± 3.7			6.43 ± 0.07	0.96 ± 0.01	14.45 ± 0.09
				$10° \leq \|b\| \leq 80°$				
0	1.74 ± 0.02	5.31 ± 0.12				7.90 ± 0.09	0.98 ± 0.01	12.40 ± 0.10
284.4	***1.74 ± 0.02***	***5.28 ± 0.12***			***4.04 ± 0.25***	***7.07 ± 0.10***	***0.97 ± 0.01***	***13.03 ± 0.10***
957.9	***1.75 ± 0.02***	***5.70 ± 0.12***		***4.32 ± 0.14***		***7.25 ± 0.09***	***0.91 ± 0.01***	***12.84 ± 0.10***
1048.6	***1.76 ± 0.02***	***5.60 ± 0.12***	***54.4 ± 1.7***			***7.17 ± 0.09***	***0.91 ± 0.01***	***12.83 ± 0.10***

Grenier, Casandjian & Terrier, Science 307, 1292 (2005)

Comparison with data

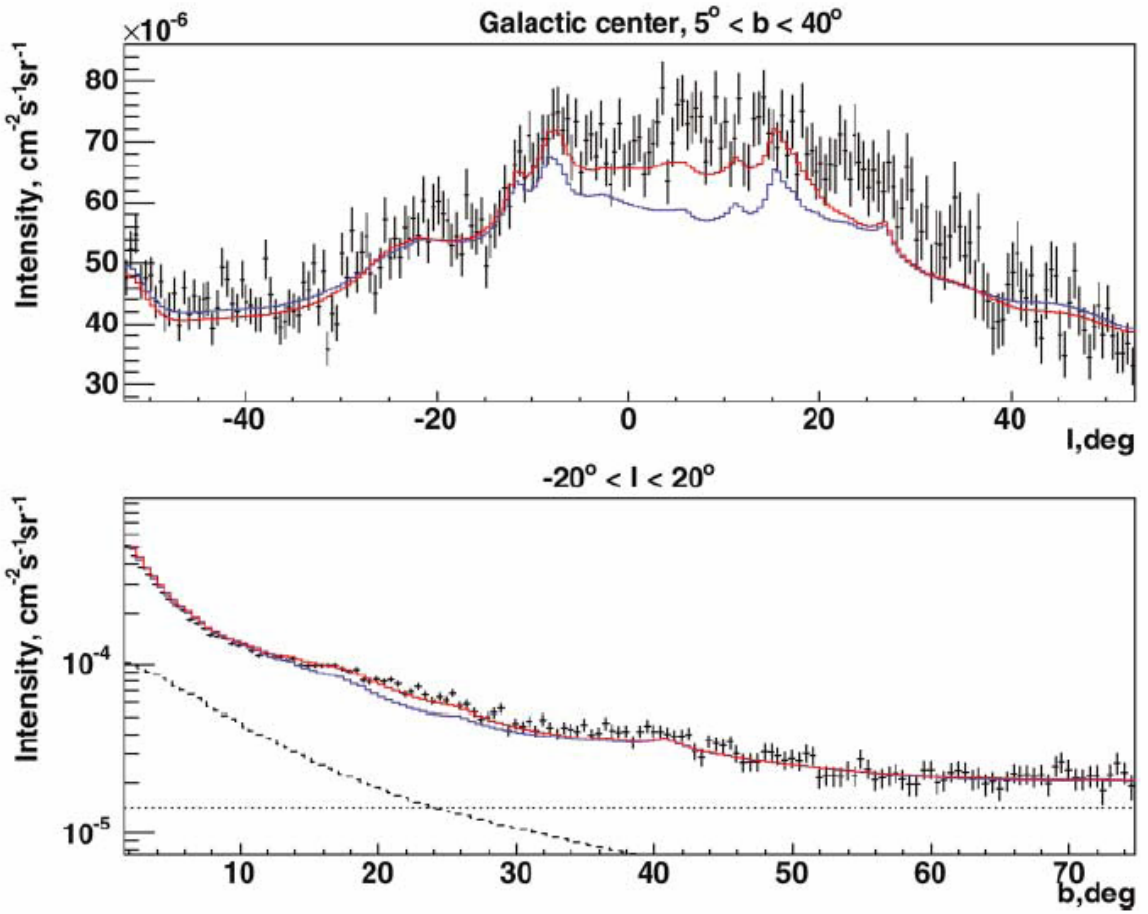

Fig. 3. Longitude (**top**) and latitude (**bottom**) profiles of the observed γ-ray intensity in the Aquila-Ophiuchus-Libra region versus the N(HI)+W(CO) gas model (blue) and the N(HI)+W(CO)+E(B-V) model (red). The dashed and dotted curves (bottom) outline the IC and extragalactic background intensities, respectively. Error bars show mean ± SD.

Grenier, Casandjian & Terrier, Science 307, 1292 (2005)

Dark gas distribution based on the fit

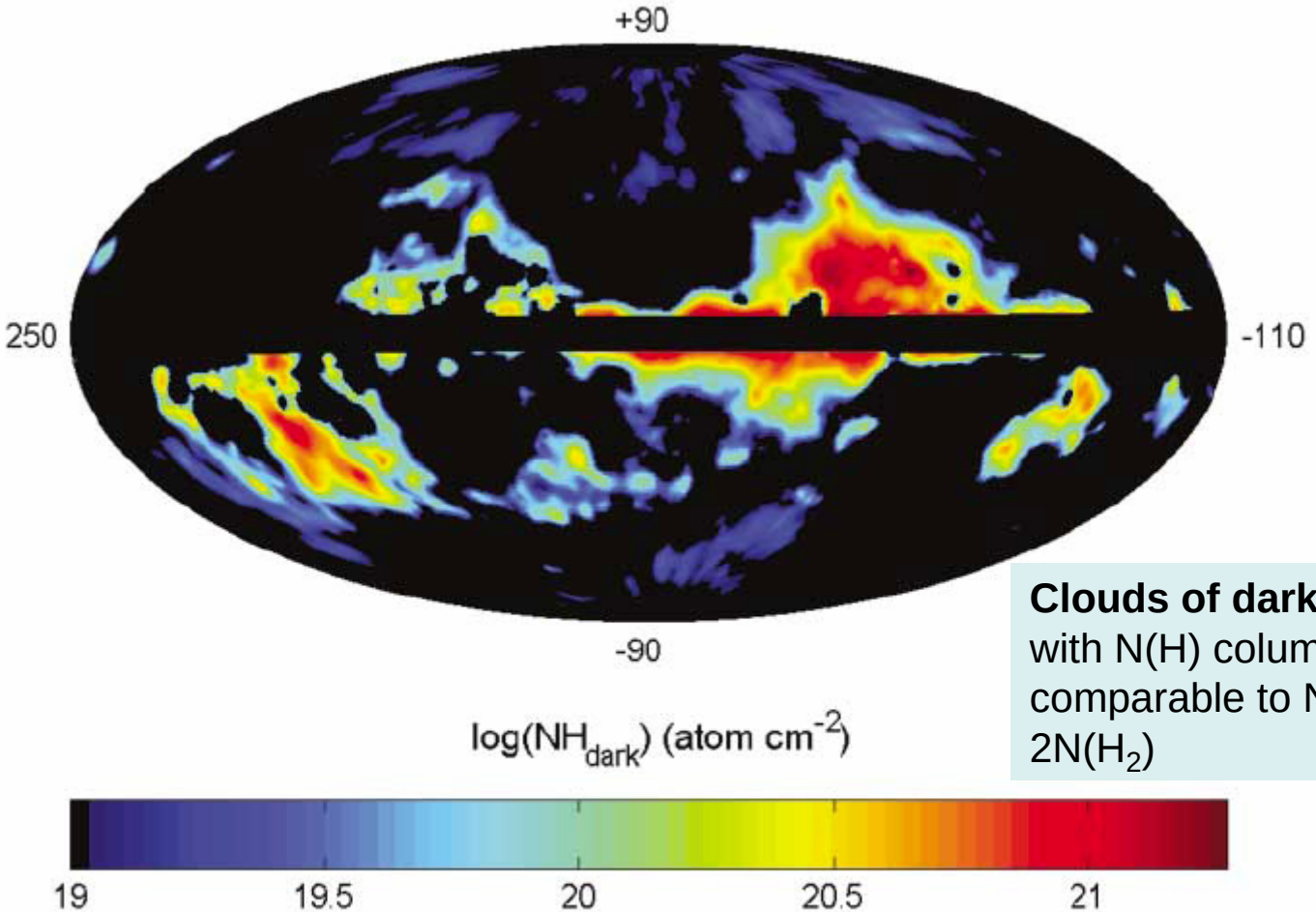

Fig. 4. Map, in Galactic coordinates centered on $l = 70°$, of the column densities of dark gas found in the dust halos, as measured from their γ-ray intensity with the reddening map. This gas complements that visible in HI and CO. The two dust tracers [E(B-V) and 94-GHz emission] yield consistent values within 30% over most regions.

Clouds of dark gas (39 σ)!
with N(H) column-densities comparable to N(HI) and 2N(H_2)

Grenier, Casandjian & Terrier, Science 307, 1292 (2005)

Latitude profile

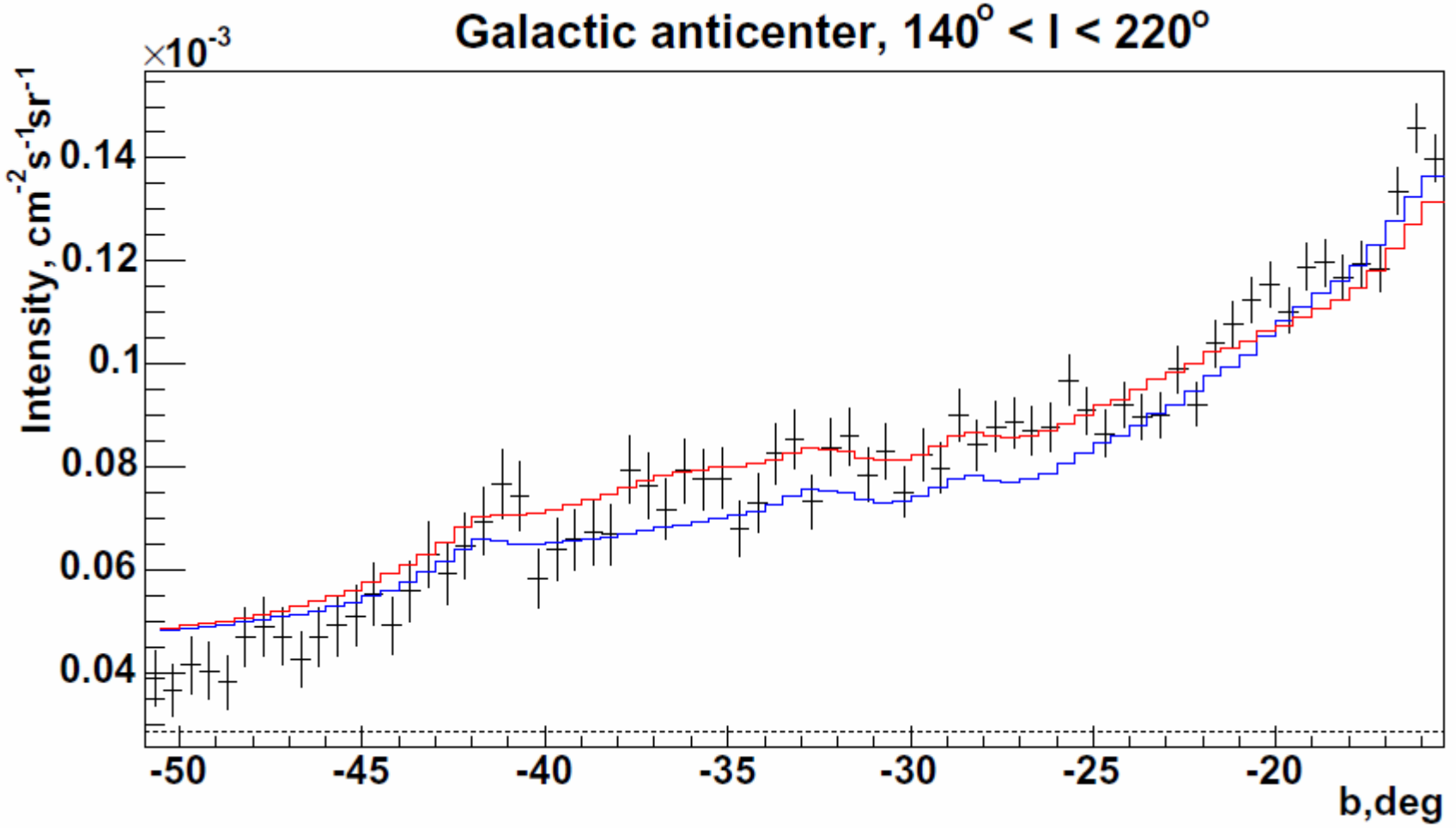

Fig. S1. Latitude profile of the observed γ-ray intensity in the Taurus-Perseus-Triangulum region versus the N(HI)+W(CO) gas model (blue) and the N(HI)+W(CO)+E(B-V) model (red). The dotted line notes the extragalactic background intensity.

Nearby dark gas clouds

Table 2. Total mass and H_2:dark:HI mass proportions in the CO, dark, and atomic phases in nearby regions.

Region	Longitudes, latitudes	Distance (pc)	Total mass ($10^5\ M_\odot$)	H_2:dark:HI
Cepheus-Cassiopeia-Polaris	[80,165] [5, 50]	300	5.4	7.5:1:7.3
Orion	[–163, –134] [–40, –5]	450	4.8	8.6:1:7.3
Aquila-Ophiuchus-Libra	[–70, 50] [5, 60]	140	1.6	0.8:1:1.0
Taurus-Perseus-Triangulum	[140, 197] [–60, –5]	140	1.4	2.3:1:3.1
Aquila-Sagittarius	[–36, 50] [–50, –5]	140	0.43	0.2:1:0.5
Chamaeleon	[–90, –35] [–50, –8]	160	0.40	0.9:1:3.7
Pegasus	[50, 140] [–60, –26]	150	0.16	0.7:1:3.4

H_2 mass vs. dark mass: evolution?

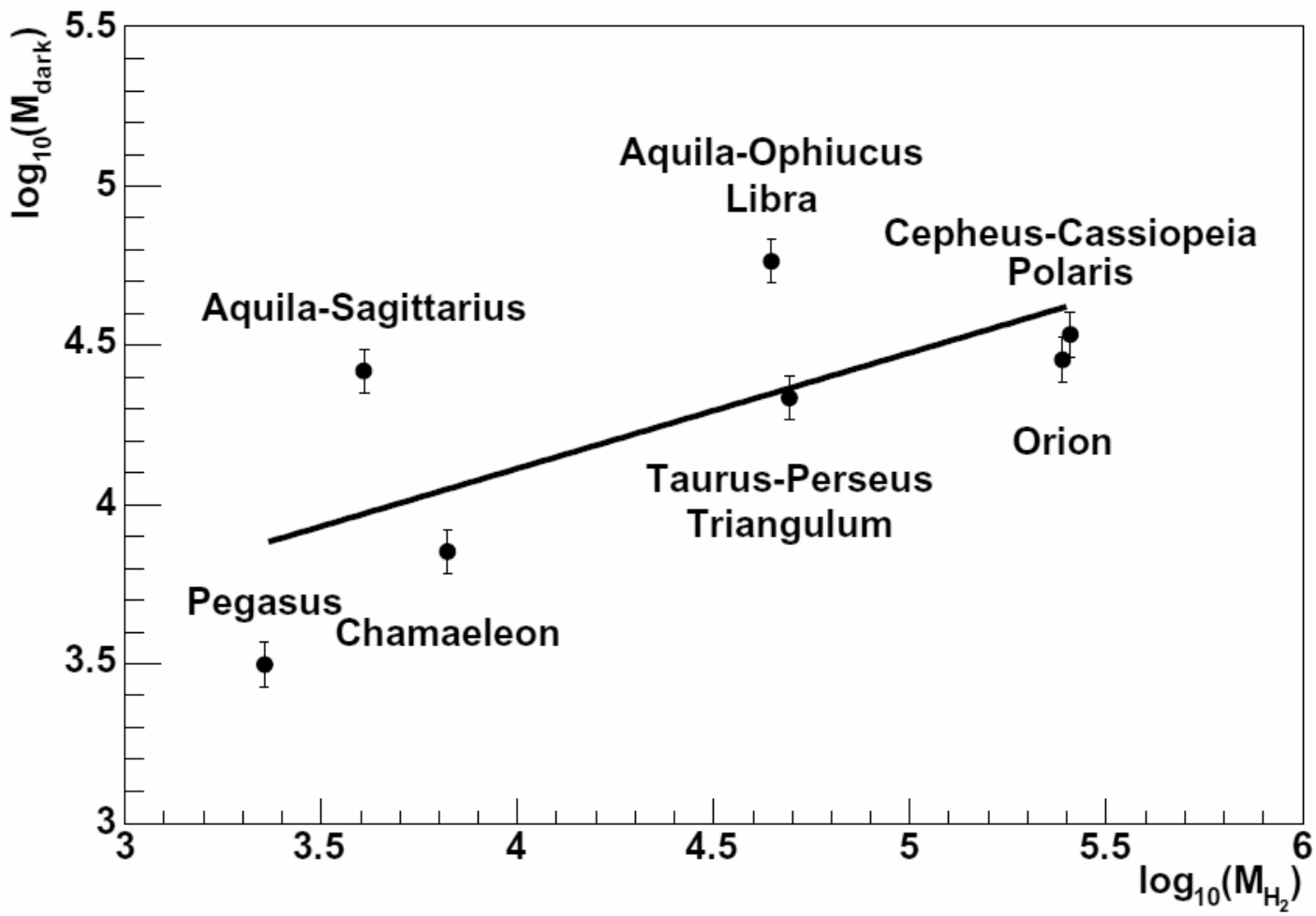

Fig. S3. Evolution of the dark-gas mass with the H_2 mass in the CO clouds for the seven local regions, in solar masses, using $X_\gamma = (1.74 \pm 0.03)\ 10^{20}$ cm^{-2} K^{-1} km^{-1} s.

Grenier & Casandjian, Paleisaeu workshop (April, 2005)

Model comparison

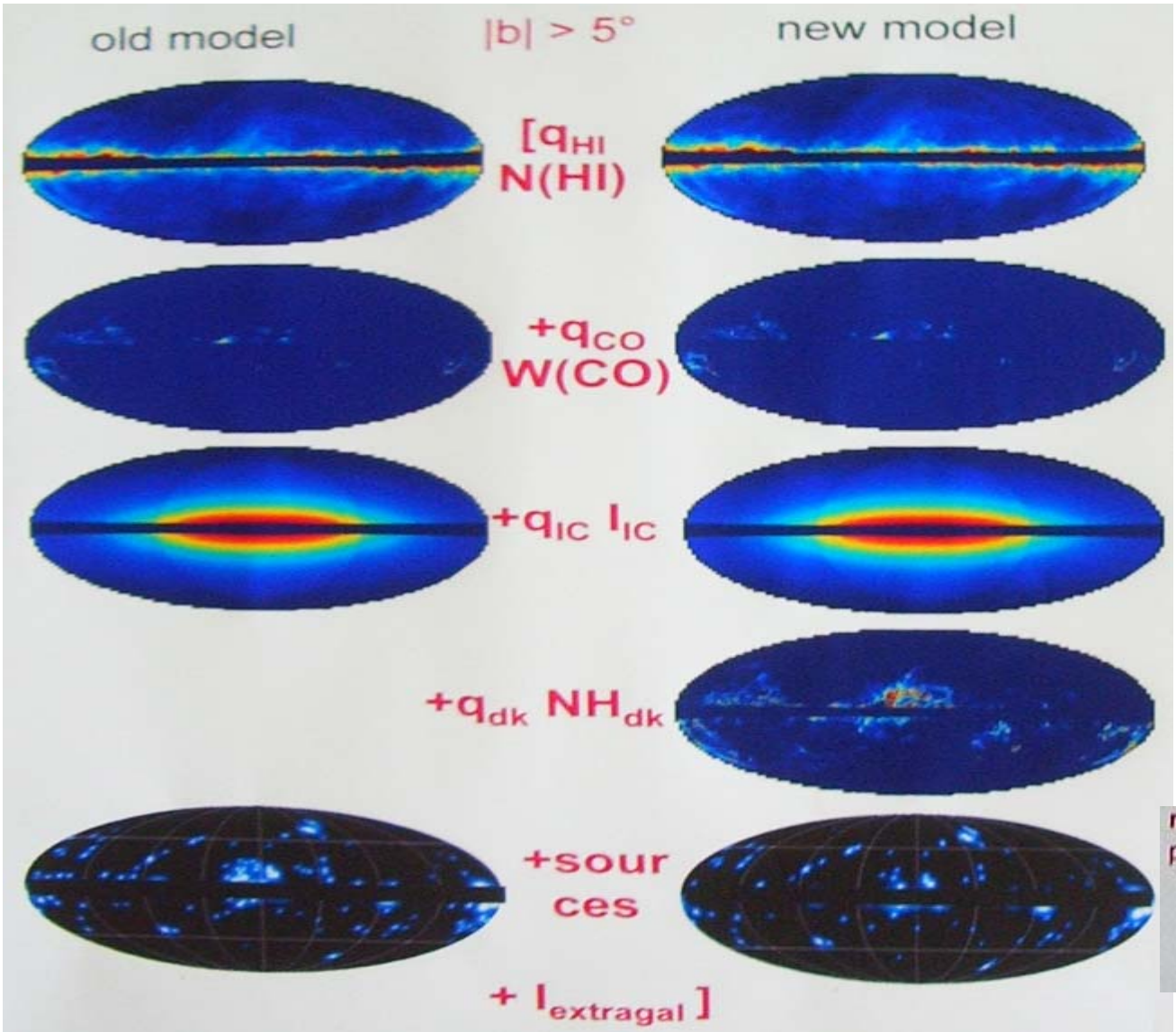

× **exposure**

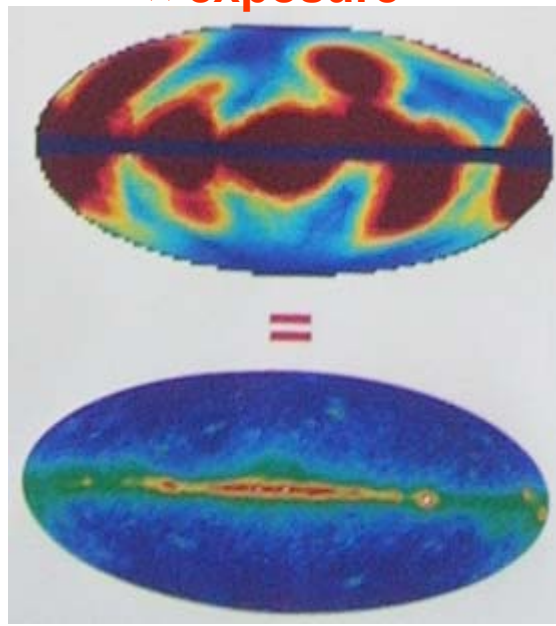

new EGRET source detection:
preliminary results; many 3EG sources toward the dark clouds do not meet the 4-5 σ threshold requirement over the new interstellar background, others have moved

Casandjian, Grenier & Terrier, ICRC OG2.1 (2005)

New diffuse model

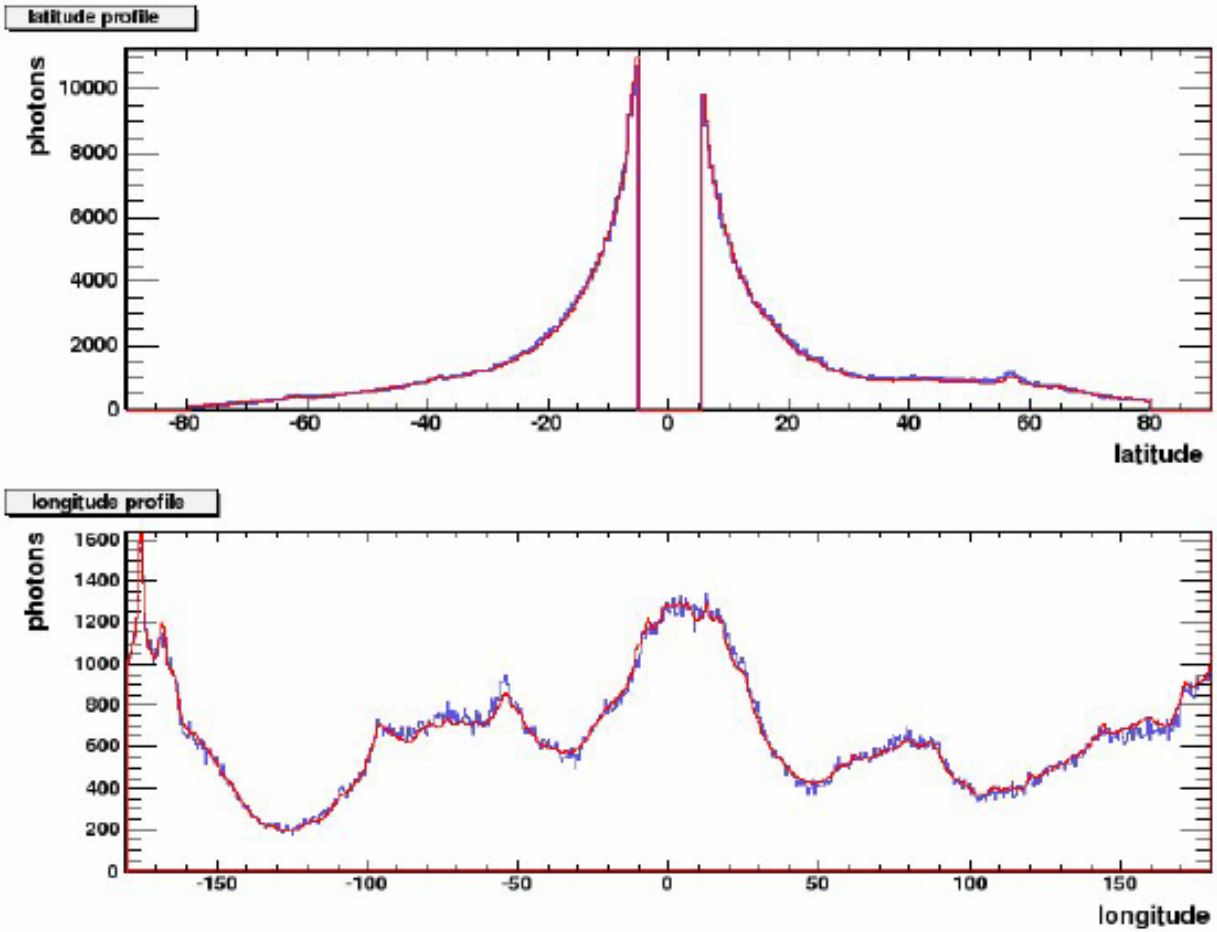

Figure 1. Latitude and longitude distributions of the EGRET photons above 100MeV. The EGRET data are in blue, our new diffuse model in red.

4. Evaluation of the method

To evaluate our method, we have first used the same interstellar emission model at all latitudes as for the 3EG catalogue. Our analysis yields 169 persistent sources with a detection significance above 5σ at |b|<10° and 4σ at higher latitude. The 3EG catalogue lists 174 persistent ones with the same criterion, but 18 of them, very near the detection threshold, have dropped below the threshold in the new analysis or moved to a position outside the error box. Conversely, we have found 18 significant sources that are not listed or have a different position in the EGRET catalogue. To compare positions, we have used a match test with a completeness of 99%. If we release this criterion and allow a slight shift in position, the number of 3EG sources without a match falls to 11, among which 9 were statistically weak excesses, only 0.5 σ above the threshold.

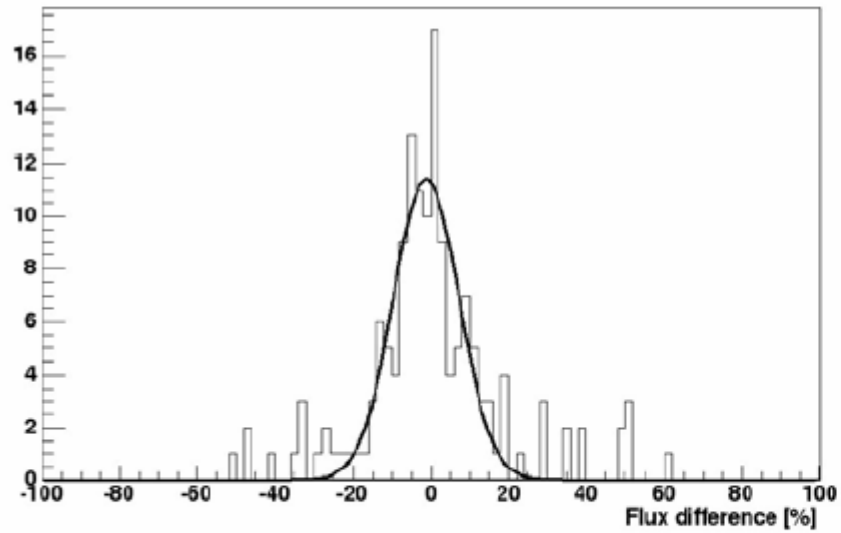

Figure 2. Relative flux difference between the 3EG and present estimates for persistent sources in cycles 1-4 at energies E > 100MeV. The Gaussian curve that best fits the distribution has an 8% dispersion.

Figure 2 shows the relative flux difference for the persistent sources between the 3EG and our estimate. This difference can be mainly attributed to the data reprocessing by the EGRET team after the catalogue was published. We indeed obtain the same distribution when we measure the 3EG source fluxes at their catalogued position with the new photons and exposure maps.

In conclusion, our method compares well with the 3EG analysis. Most of the sources were found at a consistent position and within 20% in flux. The only differences between the two source lists arise very near the detection threshold where flux variations from the reprocessed data make several sources move up or drop below the threshold. A few sources were found at a different position.

Casandjian, Grenier & Terrier, ICRC OG2.1 (2005)

EGRET unID sources

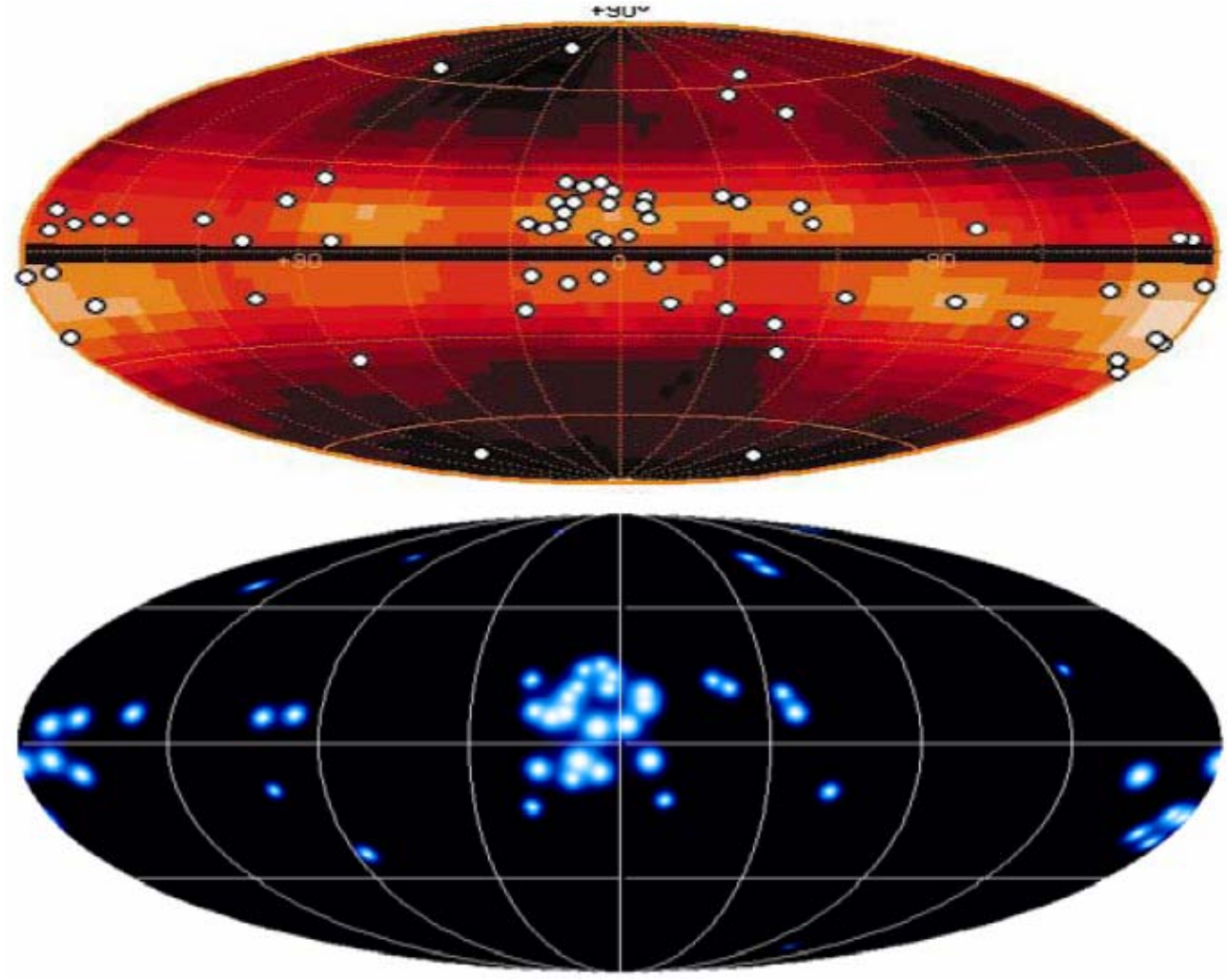

Figure 3. Distributions (in Galactic coordinates) of (a) the 67 persistent unidentified 3EG sources at |b|>2.5° and the Gould Belt [5]; (b) the 49 3EG persistent sources at |b|>5° that do not pass the detection criteria with the new diffuse emission model including the nearby dark clouds.

the Gould Belt

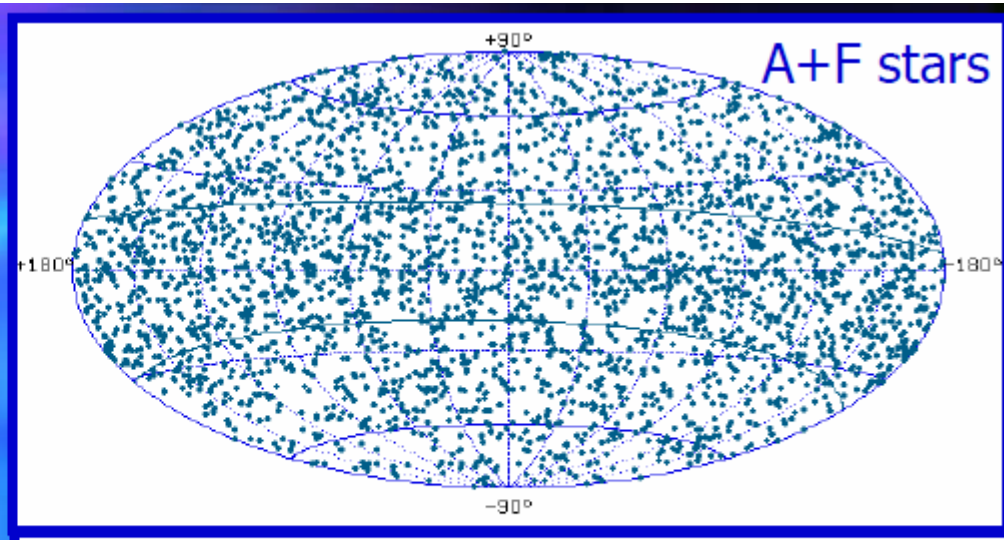

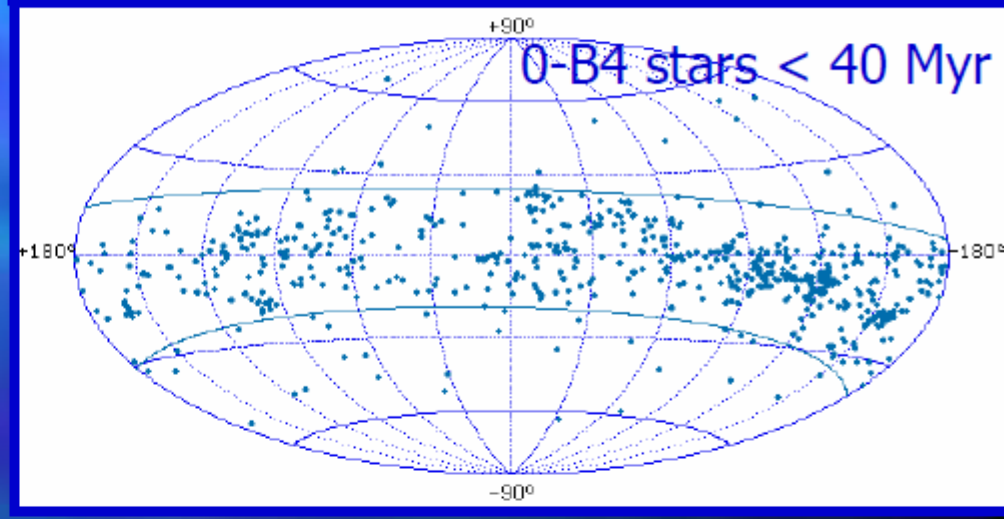

- local: D < 500 pc
  - expanding shock wave
  - Herschel (1847), Gould (1874)
- inclined: 15°-20°
- young: 20 – 80 Man
- origin ???
  - multiple SNe (Olano '82, Burton '92, Moreno '99, Pöppel '00)
  - high-v HI cloud impact (Comeron & Torra '92, '94)
  - supercloud braking in the spiral arm (Olano '01)

Grenier, XXIVth MORIOND Astrophysics (2004)

the present Gould Belt

Grenier, XXIVth MORIOND Astrophysics (2004)

$a = (373 \pm 5)$ pc, $b = (233 \pm 5)$ pc

$i = 17.2° \pm 0.3°$

$E_{ini} = (1.0 \pm 0.1)\ 10^{45}$ J: 10 SNe or GRB

age = (26.4 ± 0.4) Myr

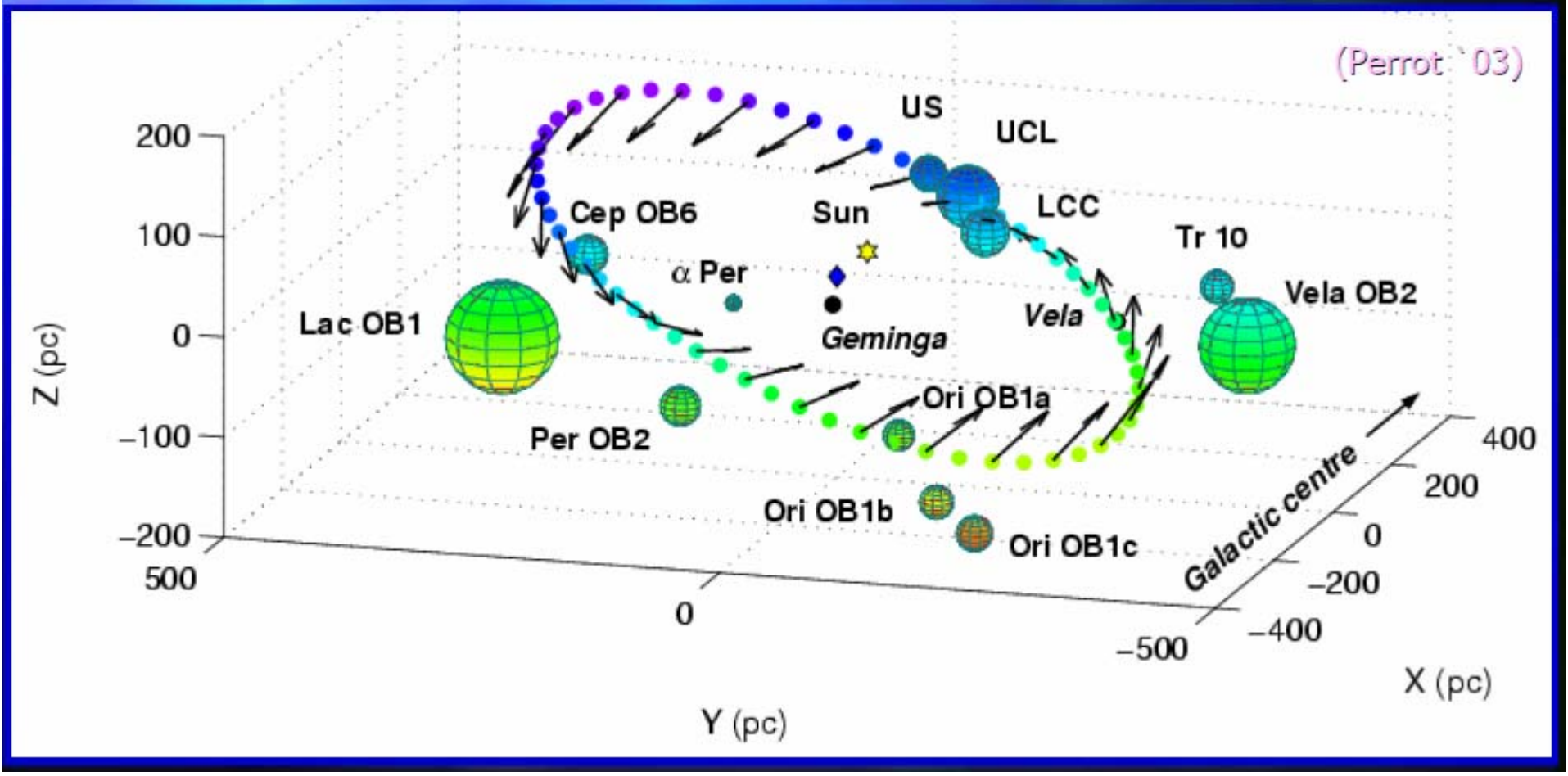

γ-ray sources

40 ± 5 associated with Belt

L_γ = 0.2-8 10^{26} W (D/300 pc)²

stable

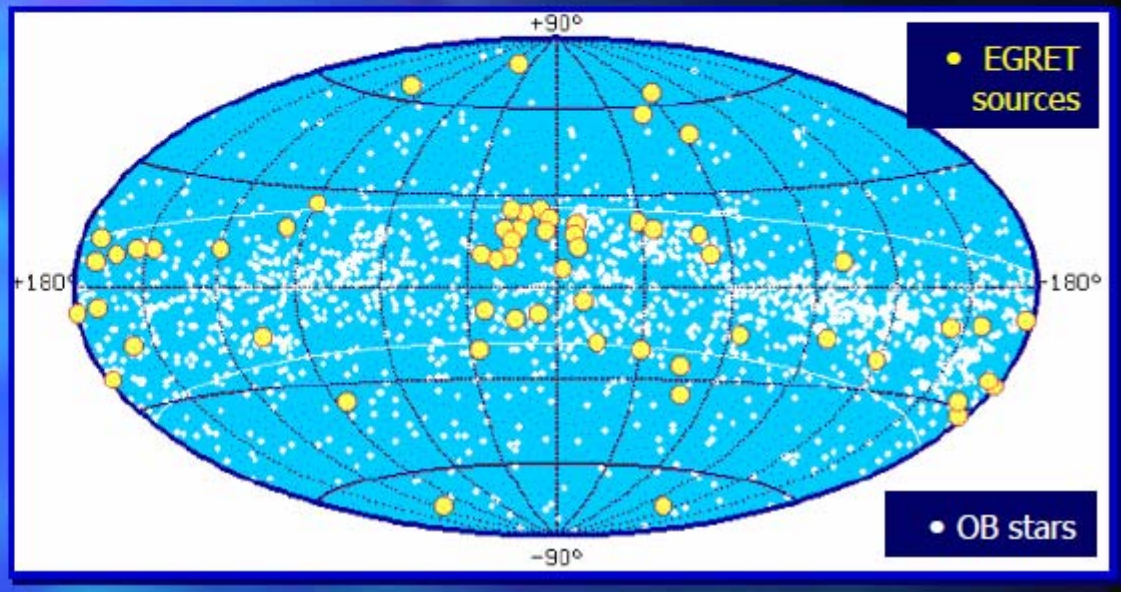

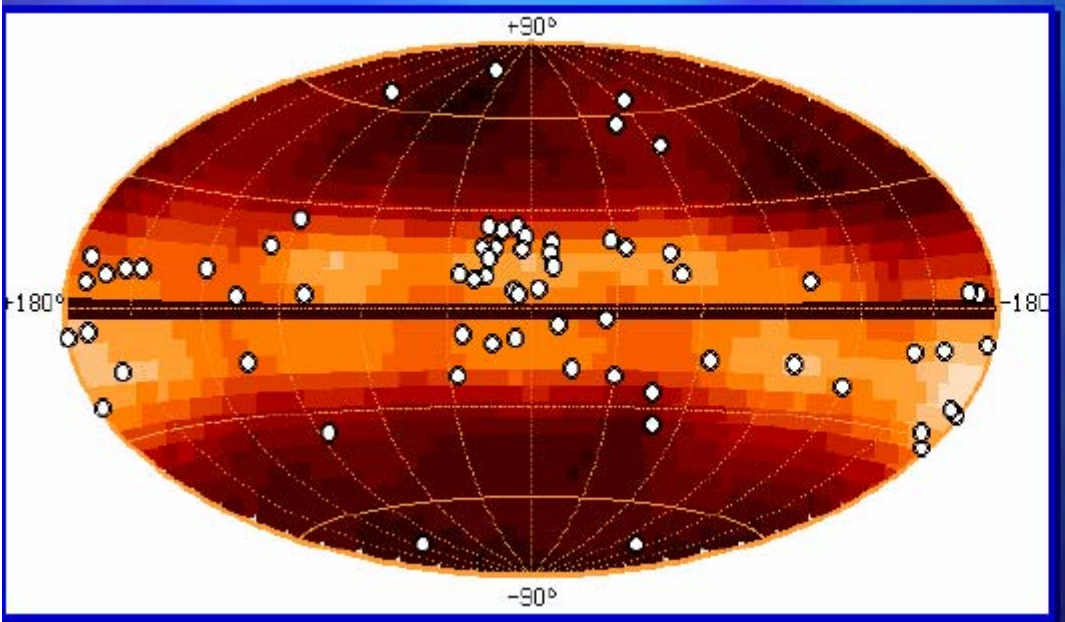

not unresolved clouds 10^4 M⊙

not Belt SNR (too extended)

no O-early B star in boxes

not accreting systems

pulsars ?

(Grenier '00)

Grenier & Casandjian, GLAST meeting (Aug. 2005)

Model comparison

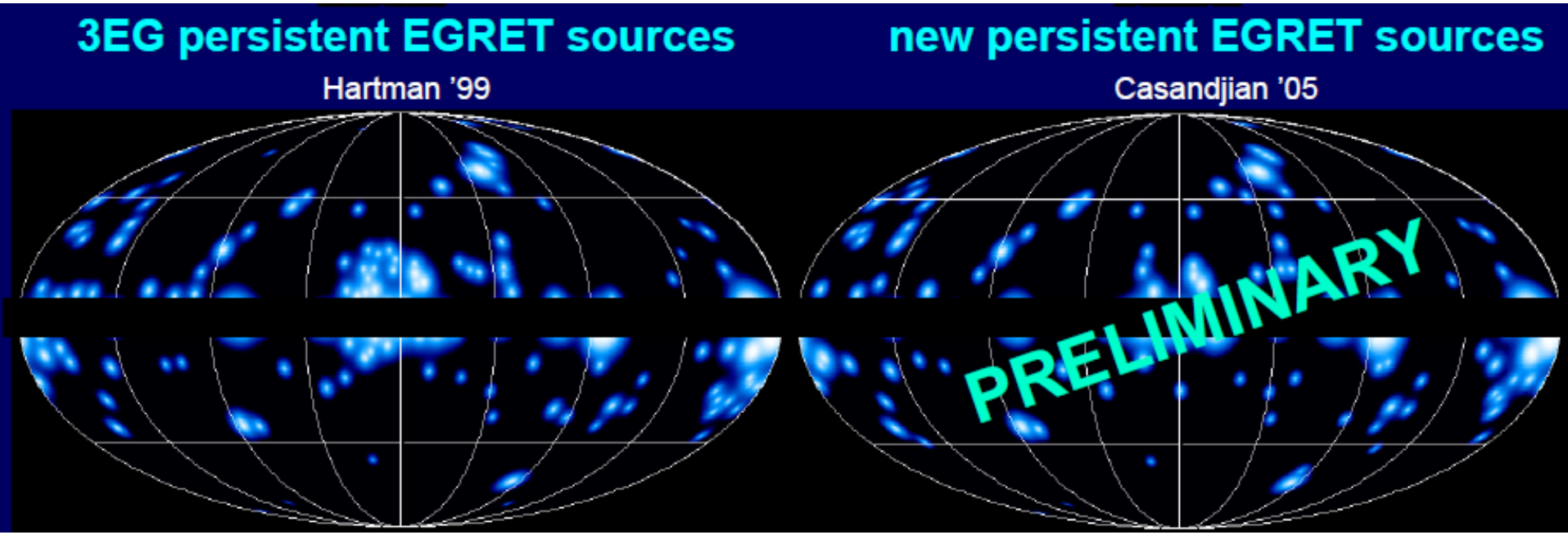

Summary

- New interstellar emission model that includes the local dark clouds were developed.
- Mass of local dark clouds is comparable to that of molecular clouds.
- With the new interstellar background, only several new sources appeared and most of the persistent unidentified sources associated with the Gould Belt lost their significance.